Design and Experimental Evaluation of a Piezoelectric XY Stage

F. Barillot, R. Le Letty, F. Claeyssen, N. Lhermet, Cedrat Recherche

M. Yorck, SI IKOSS B.V.

P. Bouchilloux, Magsoft

The ROSETTA/MIDAS mission of the European Space Agency (ESA) intends to study the dust collected from the Wirtanen comet using an Atomic Force Microscope (AFM) (Figure 1). This instrument utilizes an XY piezoelectric stage to achieve precise positioning in two in-plane orthogonal directions, and a Z actuator to support the needles for the analysis of dust particles in the out-of-plane direction.

Even though several types of piezoelectric actuators have already been used in other instruments sent into space, they were never used in combination with an AFM. In the case of the ROSETTA/MIDAS positioning stage, several degrees of freedom had to be controlled according to the following requirements:

- strokes of 100 μm for scanning along both the X and Y directions
- stroke of 8 μm along the Z direction
- reduced parasitic rotations (as small as possible) about the axes X, Y and Z
- a maximum total of three independent electric ports for all X, Y and Z strokes

Cedrat Recherche designs and produces a new type of piezoelectric actuators, called Amplified Piezoelectric Actuators (APA). These actuators do not display the usual weak points found in amplification mechanisms such as flexural hinges. Also, the elastic amplifiers of the APAs can be used to directly prestress the Ceramic Multilayer Actuators (CMAs), thus preventing the CMAs from working in tensile stress. This results in a gain of mass in the final system, since APAs are usually lighter than other amplified actuators that require external prestress mechanisms.

These APA actuators were chosen as the base components of the stage, because they seemed to provide, on top of the required characteristics in terms of stroke and robustness, a simpler and easier construction than competing technologies. The easier construction would, in particular, permit the careful integration of the capacitive sensors into the assembly. The general concept of the stage is shown in Figure 1. APA actuators are used in the X and Y directions to provide the required strokes. They also act as the necessary guiding functions by forming a regular parallelogram. Flexural hinges are used to decouple the X and Y axes, which are identical for reasons of symmetry. These hinges were preferred to Hertzian pivots because the pivots could lead to tribological problems in the space environment. Z stiffeners are used to correct the parasitic rotations induced about the X and Y axes.

The required angular deviations were also considered to be a serious difficulty, which could not be handled independently from the global design of the stage. Later in the project, the X and Y parasitic rotations appeared as a key point of the design, and it

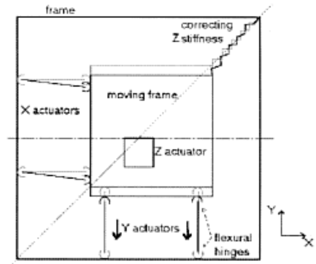

Figure 1. Basic principle of the XY stage

was requested that they be kept below 12 μrad. This value is lower than that reached in current commercial products.

The design phase required the use of CAD and FEA software packages, namely IDEAS-SDRC and ATILA. These programs were used to define the stage and its components, as well as to verify the viability of the design through an extensive use of finite element models. These packages also permitted the prototype to be fabricated using computer numerical control (CNC) and electrodischarge machining (EDM) techniques.

The testing phase for this initial prototype took place at Cedrat Recherche's laboratory. The thermal and lifetime tests were successful, but the stage was not able to pass the vibration levels imposed by the project requirements.

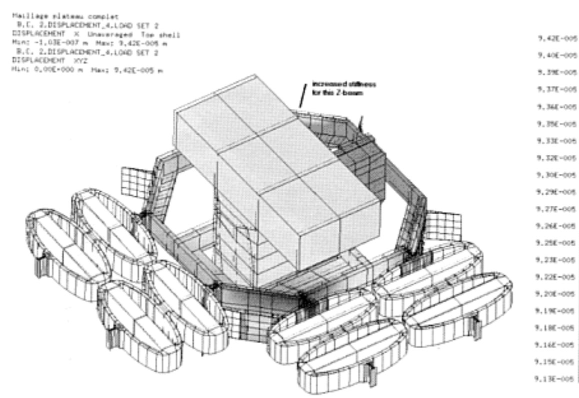

Figure 2. Static excitation of the X actuators under 200V (ATILA FEM results)

Finally, the implementation of a latch mechanism was studied. A second prototype of the stage was built with the latch mechanism and is discussed in a separate publication.

As previously mentioned, both the ATILA and IDEAS-SDRC software packages were used to design the stage, combined with theoretical calculations. ATILA was used for the finite element analysis of the piezoelectric actuation mechanisms while IDEAS-SDRC was used for standard mechanical analyses of the stage. The stage shape and dimensions were defined from the ATILA models. These models also provided performance estimates from various standpoints. For instance, the static analyses computed the actuators' stroke and capacitance (Figure 2). Modal analyses provided information about the vibration modes in terms of frequencies, mode shapes, effective electromechanical coupling factors, and stress levels associated with the amplitudes of the vibrations. These modal analyses allowed determining all the electromechanical properties of the stage. They were also helpful in determining, through the mechanical quality factor of the modes, the various stiffnesses of the system parts and their resistance to launching vibrations.

Mechanisms based on piezoelectric actuators require that special attention be paid to the guiding functions. In most cases, these functions are accomplished by elastic mechanisms whose presence reduces the actuation performance in the form of stored uncoupled elastic energy. Such effects can be accounted for by using for the actuator assembly a coefficient k_t defined as:

$$k_t = \frac{k_a}{k_a + k_g}$$

where k_a, k_g are the stiffnesses of the actuator and the elastic guide. The piezoelectric actuator's stroke is reduced in proportion to the k_t coefficient due to the guiding.

The front and back views of the initial stage prototype are shown in Figures 3 and 4. The frame is made of stainless steel, fabricated using CNC and EDM techniques. The XY stage is excited using Cedrat Recherche's SA75 electronic drives, and its operating performance measured using a dedicated test bench. This test bench includes capacitive sensors that are used to measure the X and Y strokes versus input voltage, the hysteretic open loop response in the X and Y directions, and the cross-coupling between the two axes. The test bench also includes a laser interferometer to measure the rotations about the X, Y, and Z axes.

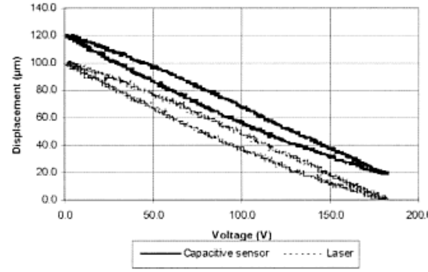

Figure 5. Hysteresis measurement when the stage's X axis is excited (the laser measurement is offset for a clearer view)

The responses from the capacitive sensors and the laser interferometer were compared and found to be very similar (Figure 5). The linearity error on the system is less than 0.5% and hidden in the measurement noise due to the sampling resolution, the laser drift and parasitic ground vibrations.

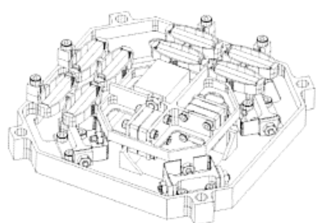

Figure 3. Front view of the stage

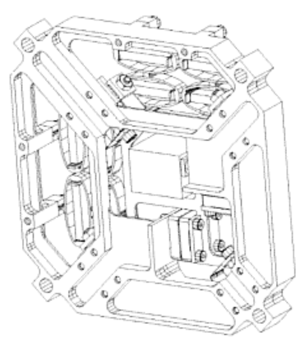

Figure 4. Back view of the stage

Some observations from the tests are:

- The discrepancies between the two X and Y axes (on the order of 1%) seem directly related to the different behavior of the actuators
- The strokes found are similar to those predicted (110 µm at room temperature)
- The ratio between the no-load actuator displacements and the stage displacements corresponds to the k_t coefficient, which is also the ratio between the actuator's stiffness and the parallel stiffness, is comparable to the predicted values (0.88)
- The Z rotations (25 arcsec) meet the specifications, but must be optimized
- The X and Y rotations, though not specified, are comparable to the typical values of commercially available products
- The cross-coupling between the X and Y axes measured on the sensors is less than 2 %.

The thermal range tested was -20 to +50C. The stroke found at -10C was 106 µm; at 40C, 115 µm. The total change of dimensions over the whole working temperatures range (50C) is 46.8 µm. This results in a correction of 4.68V for the zero sensor responses. This effect had to be taken into account for both the assembly and the design of the latch mechanism. In particular, reducing the thermo mechanical effects was possible by reducing the thermo mechanical mismatch between the CMAs (with a thermal expansion coefficient (α =

3.5e-6/K) and the actuator's shell material (α = 10.8e-6/K, initially).

The stage was submitted only to low level random vibrations (1g) to compare its response (Figure 7) with the model predictions. Both the acceleration levels on the payload and the voltages appearing on the electrical ports were measured. The agreement between predictions and measurements is satisfactory, in general. It appears that the vibration modes are not all equally damped and, although elastomeric mounts have been used, some modes display a quality factor of 60 or more, which is undesirable. The translation and the rotation of the payload on the Z axis are more coupled than predicted for reasons that remain unclear (perhaps because of the presence of the accelerometer cable on the payload).

The stage did not show any significant changes during the tests (1.25e6 cycles). The variations are due to the room temperature, which was 20 +/-1 C, and influence the zero sensor response (0.9 µm/K), and to the gain drift of the SA75 drives (estimated to 0.1 %/K).

The design of the stage cannot be separated from the design of the piezoelectric actuators and the integration requirements for capacitive sensors, which make it necessary to maintain accurate distances between the two sensor parts. Furthermore, the design of the stage is also strongly influenced by the implementation of the latch mechanism.

Due to both the small mass budget (and consequently limited stiffness) and the requirements on the sensors, the stage is sensitive to three factors in particular: mounting, gravity, and temperature.

The required operating performance was achieved. The angular deviation about the Z axis was measured within the required envelope without supplementary work. However, our models showed possible optimization of the Z beam shape that would reduce this angular deviation even further.

The thermo mechanical behavior of the stage is not optimized since the amplified piezoelectric actuators APA50S themselves have an expansion of -0.5 µm/K, due to the thermo mechanical mismatch between the CMA and the steel of the shell.

The mismatch between the actuation behavior in the two directions can be resolved by carefully selecting the CMAs. However, these actuators display high quality factors requiring the introduction of damping materials into the system. These damping materials will preferably be included in the guiding system so as to avoid the additional errors in the guiding function that would occur if elastomeric mounts were to be added instead.

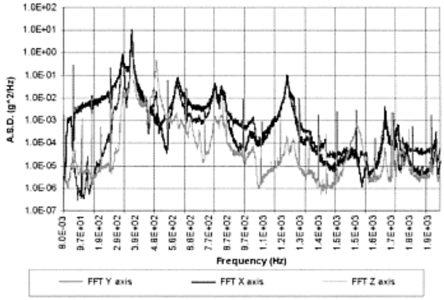

Figure 7. Acceleration spectral density (ASD) leve (g3/Hz) on the X axis excitation

The finite element models correctly predicted the functional and modal behaviors of the stage:

- The modes are predicted with an error less than 5%
- The actuator strokes were correctly estimated; however, since corrections of the contact stiffness inside the actuator were performed later in the process, the models should be updated
- Parasitic displacements are correctly reproduced (e.g., the X-Y rotations)
- The clamping of the Z-beam stiffeners is overestimated by the model
- The thermo mechanical model gives a reasonable representation of the system's behavior

The mechanism presented in this paper, based on piezoelectric actuators, contains 6 degrees of freedom: 3 of them must be actively controlled and the other 3 must be passively cancelled. Specific characteristics of this device are the low mass budget allowed and the high strokes required, which cannot be attained with conventional direct piezoelectric actuators.

The extensive use of finite element models, which have proven to accurately represent the system, greatly facilitated the design. As a result, the operating performance was obtained with the first prototype built.

Thermal and lifetime tests showed that the instrument's operating performance did not degrade beyond the required limits. Therefore, the technology can be considered mature for this new space mission.

A second prototype was built with a latch mechanism, thus adding to the stiffness of the entire stage. This second prototype successfully passed the vibration tests and will be discussed in a separate publication.

ACKNOWLEDGEMENTS

This work was performed under ESA TRP contract N13090/98/NL/MV. The authors gratefully acknowledge the European Space Agency.

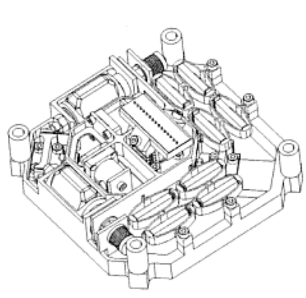

Figure 8. View of the final stage including the latch mechanism (locked)